

# Lawrence Berkeley National Laboratory

## Recent Work

### Title

IPTF SEARCH for AN OPTICAL COUNTERPART to GRAVITATIONAL-WAVE TRANSIENT GW150914

### Permalink

<https://escholarship.org/uc/item/5tp05351>

### Journal

Astrophysical Journal Letters, 824(2)

### ISSN

2041-8205

### Authors

Kasliwal, MM  
Cenko, SB  
Singer, LP  
[et al.](#)

### Publication Date

2016-06-20

### DOI

10.3847/2041-8205/824/2/L24

Peer reviewed

## iPTF SEARCH FOR AN OPTICAL COUNTERPART TO GRAVITATIONAL WAVE TRIGGER GW150914

M. M. KASLIWAL<sup>1</sup>, S. B. CENKO<sup>2,3</sup>, L. P. SINGER<sup>2,4</sup>, A. CORSI<sup>5</sup>, Y. CAO<sup>1</sup>, T. BARLOW<sup>1</sup>, V. BHALERAO<sup>6</sup>, E. BELLM<sup>1</sup>, D. COOK<sup>1</sup>, G. E. DUGGAN<sup>1</sup>, R. FERRETTI<sup>7</sup>, D. A. FRAIL<sup>8</sup>, A. HORESH<sup>9</sup>, R. KENDRICK<sup>10</sup>, S. R. KULKARNI<sup>1</sup>, R. LUNNAN<sup>1</sup>, N. PALLIYAGURU<sup>5</sup>, R. LAHER<sup>11</sup>, F. MASCI<sup>12</sup>, I. MANULIS<sup>9</sup>, A. A. MILLER<sup>1,13,14</sup>, P. E. NUGENT<sup>15,16</sup>, D. PERLEY<sup>17</sup>, T. A. PRINCE<sup>1</sup>, R. M. QUIMBY<sup>18,19</sup>, J. RANA<sup>6</sup>, U. REBBAPRAGADA<sup>13</sup>, B. SESAR<sup>20</sup>, A. SINGHAL<sup>6</sup>, J. SURACE<sup>11</sup>, A. VAN SISTINE<sup>21</sup>

<sup>1</sup>Cahill Center for Astrophysics, California Institute of Technology, Pasadena, CA 91125, USA

<sup>2</sup>Astrophysics Science Division, NASA Goddard Space Flight Center, Code 661, Greenbelt, MD 20771, USA

<sup>3</sup>Joint Space-Science Institute, University of Maryland, College Park, MD 20742, USA

<sup>4</sup>NASA Postdoctoral Program Fellow

<sup>5</sup>Texas Tech University, Physics Department, Lubbock, TX 79409-1051, USA

<sup>6</sup>Inter-University Centre for Astronomy and Astrophysics (IUCAA), Post Bag 4, Ganeshkhind, Pune 411007, India

<sup>7</sup>The Oskar Klein Centre, Department of Physics, Stockholm University, SE-106 91 Stockholm, Sweden

<sup>8</sup>National Radio Astronomy Observatory, Socorro NM

<sup>9</sup>Department of Particle Physics and Astrophysics, Weizmann Institute of Science, 76100 Rehovot, Israel

<sup>10</sup>Lockheed Martin Space Systems Company, Palo Alto, CA

<sup>11</sup>Spitzer Science Center, California Institute of Technology, M/S 314-6, Pasadena, CA 91125, U.S.A.

<sup>12</sup>Infrared Processing and Analysis Center, California Institute of Technology, Pasadena, CA 91125, USA

<sup>13</sup>Jet Propulsion Laboratory, California Institute of Technology, Pasadena, CA 91109, USA

<sup>14</sup>Hubble Fellow

<sup>15</sup>Astronomy Department, University of California at Berkeley, Berkeley, CA 94720, USA

<sup>16</sup>Lawrence Berkeley National Laboratory, 1 Cyclotron Road MS 50B-4206, Berkeley, CA 94720, USA

<sup>17</sup>Dark Cosmology Centre, Niels Bohr Institute, Juliane Maries Vej 30, Copenhagen , DK-2100, Denmark

<sup>18</sup>San Diego State University, San Diego CA

<sup>19</sup>Kavli IPMU (WPI), UTIAS, The University of Tokyo, Kashiwa, Chiba 277-8583, Japan

<sup>20</sup>Max Planck Institute for Astronomy, Königstuhl 17, D-69117 Heidelberg, Germany

<sup>21</sup>Department of Physics, University of Wisconsin-Milwaukee, Milwaukee, WI 53201, USA

### ABSTRACT

The intermediate Palomar Transient Factory (iPTF) autonomously responded to and promptly tiled the error region of the first gravitational wave event GW150914 to search for an optical counterpart. Only a small fraction of the total localized region was immediately visible in the Northern night sky, due both to sun-angle and elevation constraints. Here, we report on the transient candidates identified and rapid follow-up undertaken to determine the nature of each candidate. Even in the small area imaged of 126 deg<sup>2</sup>, after extensive filtering, 8 candidates were deemed worthy of additional follow-up. Within two hours, all 8 were spectroscopically classified by the Keck II telescope. Curiously, even though such events are rare, one of our candidates was a superluminous supernova. We obtained radio data with the Jansky Very Large Array and X-ray follow-up with the *Swift* satellite for this transient. None of our candidates appear to be associated with the gravitational wave trigger, which is unsurprising given that GW150914 came from the merger of two stellar-mass black holes. This end-to-end discovery and follow-up campaign bodes well for future searches in this post-detection era of gravitational waves.

*Keywords:* gravitational waves, methods: observational, techniques: spectroscopic, surveys

### 1. INTRODUCTION

The direct detection of gravitational waves (GW) marks the dawn of a new era (Abbott et al. 2016b). It is widely agreed that the detection and study of the anticipated electromagnetic (EM) counterparts will vastly enrich the science returns for

the field of GW astronomy. The photometric discovery of the EM counterpart will give a precise location and a spectrum of the host galaxy will give a precise redshift. This will enable a more accurate measurement of basic astrophysical properties such as the luminosity and energetics of this strong-field gravity event. If the spectrum is timely, it may also solve the

long-standing mystery of the unknown sites of r-process nucleosynthesis.

The inherent challenge is that the two advanced GW interferometers, due to the low frequency of operation, give very poor on-sky localization (Kasliwal & Nissanke 2014; Singer et al. 2014; Berry et al. 2015; Abbott et al. 2013). Nevertheless, the prospect of finding electromagnetic counterparts by searching large sky areas is promising as the search methodology is steadily improving — from early efforts in the enhanced LIGO S6 run (Aasi et al. 2014), to proof-of-concept localizations of coarse *Fermi* gamma-ray bursts (Singer et al. 2013, 2015), to a score of EM facilities promptly responding to GW150914 (Abbott et al. 2016a).

At the time of the GW150914 trigger, there was no information disclosed on the nature of the event i.e. whether it was a binary black hole merger or binary neutron star merger or something else (GCN 18330). Many facilities undertook a search for an electromagnetic counterpart (e.g., Connaughton et al. 2016; Evans et al. 2016; Smartt et al. 2016; Soares-Santos et al. 2016). Months later, after offline analysis, the event was identified as a binary black hole merger (GCN 18858).

Here, we present the intermediate Palomar Transient Factory (iPTF) follow-up effort. iPTF uses the Samuel Oschin 48-inch telescope on Palomar mountain equipped with the CFH12K camera with a field-of-view of 7.1 deg<sup>2</sup> (Law et al. 2009). Our motivation was to look for an optical counterpart powered by free neutron decay (Metzger et al. 2015), or heavy element radioactive decay (Kasen et al. 2015; Metzger & Fernández 2014). We describe the sky area coverage, candidate identification, spectroscopic classification and panchromatic follow-up. We conclude with our plans for a way forward.

## 2. IDENTIFYING CANDIDATES

On UT 2015 September 16 03:17, the iPTF Target of Opportunity Marshal automatically responded to the gravitational wave trigger alert G184098 (later named GW150914). It immediately notified the team via phone calls and SMS alerts that there had been a GW trigger. It also computed that due to the sun angle constraint and elevation constraints, Palomar would only be able to access 2.5% of the enclosed probability by tiling 126 deg<sup>2</sup> just before sunrise at high air-mass (Figure 1). This total area calculation takes into account the two non-working CCDs and the gaps between the CCDs. The small containment probability was because the southern mode of the updated (“LIB”) localization was too far south to be observable from Palomar, whereas most of the northern mode rose only after 12 degree morning twilight. Clouds did not co-operate and the Palomar 48-inch dome remained closed the first night after trigger. However, the next night (UT Sep 17), we imaged 18 fields covering this area with exposures of 1 min (See details in Table 5; GCN 18337). The scheduling and choice of tiles was further optimized applying

the algorithm described in Rana et al. 2016. A second epoch with a baseline separation of 30 min ( $\pm 1$  min) was obtained for 13 fields.

Within minutes of obtaining the data, our automated real-time image subtraction pipeline started loading candidates into our database. We have two, independent real-time pipelines – one running at the National Energy Research Scientific Computing Center (NERSC) using the HOTPANTS image subtraction algorithm (Nugent et al. 2015) and the other running at the Infrared Processing and Analysis Center (IPAC) using the PTFIDE algorithm (Masci 2016). Due to the dynamic nature of the optical sky, the candidate list was dominated by false positive transients unrelated to the gravitational wave trigger. A total of 127676 candidates were loaded into the NERSC database and 32576 in the IPAC database. Our automated machine-learning-aided filtering algorithms rejected the moving objects in our solar system, variable stars in the Milky Way as well as subtraction artifacts. A list of 13 candidates were presented on a dynamic web portal for human vetting.

We have been refining our software algorithms that quickly sift through the large number of candidates during our *Fermi* Gamma-ray Burst Monitor afterglow search effort (Singer et al. 2015). The EM-GW challenge has some similarities and some differences. The similarities are that we need to continue to reject foreground asteroids/variable stars and background supernovae/active galactic nuclei. The differences are that compared to a Gamma Ray Burst afterglow, the EM-GW counterpart may be relatively fainter and/or slower and/or redder. Knowing that the EM counterpart is relatively nearby due to the advanced LIGO sensitivity helps further reduce false positives.

The following are some rejection criteria:

1. Movement in detections in two epochs separated by at least 15 min suggesting the candidate is an asteroid
2. Past history of eruption in PTF/iPTF data (baseline of six years) suggesting the candidate is an old transient
3. Previously known radio source or X-ray source suggesting the candidate is an active galactic nucleus
4. Previously known optical or infrared point source underneath the position suggesting the candidate is a stellar flare

The following criteria lead to flags for follow-up spectroscopy, additional photometry and/or multi-band follow-up:

1. Host galaxy (within 100 kpc of transient) with spectroscopic redshift  $< 0.05$  (or photometric redshift  $< 0.1$ ) — this is motivated by advanced LIGO’s sensitivity limit to binary neutron star mergers
2. Photometric evolution on hour timescale ( $> 0.2$  mag) or day timescale ( $> 0.5$  mag) or one-week timescale

(>1 mag) — this serves as a strong discriminant against old supernovae. We note that this flag was not applied for GW150914 as all candidates of interest were spectroscopically classified within two hours.

3. Hostless candidates with no counterpart in deep iPTF reference co-adds — even though these are unlikely to be local, we flag these events as they are relatively rare.

To quantify the relative efficacy of each criterion, we discuss the most severe cuts in order of severity by applying each criterion independently. Of the 127676 candidates in our NERSC pipeline, only 1007 candidates (0.8% selection) are selected as being coincident with a galaxy within 200 Mpc, hence this is the most severe cut. 5803 candidates (4.5%) are selected as passing our machine learning cuts (we now have three generations of machine learning algorithms; see details in [Rebbapragada 2014](#); [Brink et al. 2013](#)). 15624 candidates (12.2%) are selected as having two detections separated by 30min in the same night. 78951 candidates (62% selection) are selected as not having an optical point source in the reference image. Similarly, in our IPAC pipeline, we had a total of 32576 candidates. Of these, 24699 did not match a star (75.8% selection), 5302 had two detections (16.2% selection) and 1964 passed our machine learning cut (6.0% selection).

In practice, these criterion are not all applied simultaneously and the candidates selected for human vetting are the result of a more complex database query. For example, prior to human vetting, we do not require coincidence with a nearby galaxy and we do not require any light curve properties. For the five fields where a second epoch was not completed on the same night, we did a manual search requiring a local universe match, found 2 candidates that were both rejected as known asteroids. After human vetting of 13 candidates, 5 candidates were rejected as they showed past history of variability in the PTF data. In summary, our team flagged 8 candidates for further follow-up in our marshal database (see [Table 5](#)). Next, we describe the prompt follow-up that was undertaken to investigate whether any of the candidates was associated with GW150914 ([GCN 18341](#)).

### 3. SPECTROSCOPIC FOLLOW-UP

Since Hawaii is west of Palomar Observatory, sunrise was three hours later and we were able to obtain spectra of all eight candidates in less than 2 hours from discovery ([Figure 2](#)). We emphasize that iPTF has routinely been obtaining spectroscopic classification on the same night as discovery, totaling 165 transients with spectra within 12 hours, thus far. We observed with the DEep Imaging Multi-Object Spectrograph (DEIMOS; [Faber et al. 2003](#)) mounted on the Keck II telescope. We used the low resolution 600 ZD grating, giving spectral coverage between 4650Å and 9600Å with a resolution of 3.5Å (full width at half maximum). Our spectra are shown in [Figure 2](#). A priori, since we searched 126 deg<sup>2</sup> to a depth of 20.5 mag, we expect  $\approx 3.2$  supernovae using the rates

in [Li et al. 2011](#) (and assuming that supernovae are brighter than  $-17$  mag for 1 month i.e. a volume out to  $z=0.075$ ).

We cross-matched our spectra with a library of supernovae spectra augmenting the `superfit` software ([Howell et al. 2005](#)). Our classifications are in [Table 5](#). We found two Type Ia supernovae (SN Ia), two hydrogen-rich core-collapse supernovae (SN II), three nuclear candidates (e.g. weak AGN where the spectrum is dominated by the host galaxy), and one hostless transient with initially unclear classification (iPTF15cyk). Offline processing of the three nuclear candidates also shows past history of photometric variability in the PTF data, which is consistent with the AGN hypothesis. The spectrum of iPTF15cyk was dominated by a blue continuum, with narrow lines suggesting a redshift of 0.539 (which would imply a very luminous transient). Since the nature of the GW source was unclear, we decided to obtain additional spectroscopic and multi-wavelength follow-up.

### 4. RADIO AND X-RAY FOLLOW-UP

We observed iPTF15cyk and the necessary calibrators with the Karl G. Jansky Very Large Array (VLA; [Perley et al. 2009](#)) in its D and DnC configurations. The observations were performed in C-band ( $\approx 6$  GHz central frequency) under our Target of Opportunity program (VLA/15A-339; PI: Corsi). VLA data were reduced and imaged using the Common Astronomy Software Applications (CASA) package. In [Table 5](#), we report the  $3\sigma$  upper-limits derived for iPTF15cyk using the full 2 GHz bandwidth ([GCN 18914](#)).

If the host galaxy redshift was confirmed, iPTF15cyk could be a super luminous supernova (SLSN) with absolute magnitude brighter than  $-22$  mag. Radio and X-ray emission from super luminous SNe may arise from interaction with the circumstellar medium (CSM; see e.g. [Ofek et al. 2013](#)). In an alternate model, superluminous supernovae could be powered by the spin-down of a nascent magnetar inside the supernova ejecta ([Kasen & Bildsten 2010](#)), which may also produce X-ray emission ([Metzger et al. 2014](#)).

However, such emission is likely to be very sensitive to the exact properties of the CSM including density profile and homogeneity. In dense CSM environments, free-free absorption can suppress the radio emission at early times. Thus, chances for a detection are maximized by observing after maximum light ([Ofek et al. 2013](#)). Hence, we observed iPTF15cyk thrice between 1 month and 4 months after discovery.

We also observed the location of iPTF15cyk with the *Swift* satellite ([Gehrels et al. 2004](#)) beginning at 18:12 UT on 2015 September 18 ( $\Delta t = 4.3$  d after the GW trigger). We do not detect any emission with the on-board X-Ray Telescope (XRT; [Burrows et al. 2005](#)) to a  $3\sigma$  limit of  $< 3.2 \times 10^{-3}$  ct s<sup>-1</sup>. Assuming a power-law spectrum with a photon index of  $\Gamma = 2$ , this corresponds to an upper limit on the unabsorbed flux (0.3–10.0 keV) of  $f_X < 1.3 \times 10^{-13}$  erg cm<sup>-2</sup> s<sup>-1</sup>.

Simultaneously we obtained images of the field with the

Ultra-Violet Optical Telescope (UVOT; [Roming et al. 2005](#)) on-board *Swift* in the  $V$ ,  $B$ ,  $U$ ,  $UVW1$ ,  $UVM2$ , and  $UVW2$  filters. No emission is detected at the location of iPTF15cyk. For a  $3''$  aperture we place the following magnitude limits (AB system) at this time:  $V > 19.29$ ;  $B > 19.81$ ;  $U > 20.62$ ;  $UVW1 > 21.61$ ;  $UVM2 > 22.27$ ; and  $UVW2 > 22.42$ . These limits were derived using the revised UV zero points and time-dependent sensitivity from [Breeveld et al. \(2011\)](#).

Additional spectroscopic follow-up of iPTF15cyk showed that it was a hydrogen-poor super luminous supernova (SLSN I; [Quimby et al. 2011](#)) at  $z=0.539$  (Figure 5), similar to LSQ12dlf at +16 d ([Nicholl et al. 2014](#)). The radio and X-ray upper limits were consistent with this classification. Given the high redshift, we concluded that this event was unrelated to GW150914. We note that the odds of finding a super luminous supernova were lower than the odds of finding other core-collapse or thermonuclear supernovae. The snapshot rate is only  $\sim 0.2$  using the volumetric rate in [Quimby et al. 2013](#) (and assuming that SLSN are brighter than  $-21$  mag for 1 month). Moreover, we have a total of only 6 events with  $z > 0.5$  (out of 2650 spectroscopically classified supernovae) in the six years of operating PTF/iPTF.

## 5. A WAY FORWARD

The post-detection era promises to be one of routine GW detections of binary neutron star mergers. With routine detections, the joint probability of  $\sim \frac{1}{3}$  that the sun ( $\sim \frac{2}{3}$ ), clouds ( $\sim \frac{2}{3}$ ), and latitude ( $\sim \frac{3}{4}$ ) simultaneously co-operate to identify the optical counterpart is not discouraging. Furthermore, given the location of Palomar Observatory in Southern California, relative to the location of the advanced LIGO interferometers, the time lag to respond is inherently less than an hour as we do not need to wait for the earth to rotate ([Kasliwal & Nissanke 2014](#)). Most of the GW150914 localization was not accessible from the Northern night sky. But, based on our simulations ([Singer et al. 2014](#)), iPTF would include the true position of the GW source for an average of  $\approx 1$  out of 2 events assuming a total of 100 iPTF observations (see Figure 4; each observation is two 60 s exposures of  $7.1 \text{ deg}^2$ ).

As advanced LIGO ramps up in GW sensitivity, we are undertaking both hardware and software upgrades to improve EM sensitivity. In 2017, we plan to commission the Zwicky Transient Facility (ZTF<sup>1</sup>; [Kulkarni 2012](#); [Bellm 2014](#)), a  $47 \text{ deg}^2$  camera on the Palomar 48-inch, with a twelve times higher volumetric survey speed than iPTF. This increase in survey speed enables a faster cadence and deeper search for the optical counterpart (e.g., 22 mag in 10 min). The larger field-of-view may also be more robust to a shifting localization (e.g. for GW150914, our enclosed probability went from 2.5% in the initial map to 0.2% in the final map; see [Abbott et al. 2016a](#)). We are continuing to improve our software algo-

rithms, e.g., better candidate filtering, image co-addition and more optimal image subtraction ([Zackay et al. 2016](#)). We are continuing to complete our census of the local universe (CLU; Cook et al. in prep) as this 200 Mpc galaxy catalog serves as the most severe filter for false positives (see examples in [Nissanke et al. 2013](#)).

Among the various models for electromagnetic emission from binary neutron star mergers, free neutron decay gives the most luminous optical counterpart (Figure 3; [Metzger et al. 2015](#)). Varying free neutron mass and opacity suggests that this counterpart may fade quickly, as much as 4 mag in 24 hours. Thus, we are also systematizing our follow-up with the Global Relay of Observatories Watching Transients Happen (GROWTH<sup>2</sup>) program. The combination of a longitudinally distributed network of telescopes as well as multi-wavelength follow-up (VLA and *Swift*) should effectively filter candidates on a 24 hour timescale. Obtaining a timely light curve, spectra and spectral energy distribution will unravel both the astrophysics and the astrochemistry of the EM counterpart. With this first gravitational wave detection, the 21st century gold rush ([Kasliwal 2013](#)) has officially begun!

Based on observations obtained with the Samuel Oschin Telescope 48-inch and the 60-inch Telescope at the Palomar Observatory as part of the intermediate Palomar Transient Factory (iPTF) project, a scientific collaboration among the California Institute of Technology, Los Alamos National Laboratory, the University of Wisconsin, Milwaukee, the Oskar Klein Center, the Weizmann Institute of Science, the TANGO Program of the University System of Taiwan, and the Kavli Institute for the Physics and Mathematics of the Universe. MMK, RL and YC acknowledge support from the National Science Foundation PIRE program grant 1545949. AAM acknowledges support from the Hubble Fellowship HST-HF-51325.01. PEN and YC acknowledge support from the DOE under grant DE-AC02-05CH11231, Analytical Modeling for Extreme-Scale Computing Environments. The National Radio Astronomy Observatory is a facility of the National Science Foundation operated under cooperative agreement by Associated Universities, Inc. AC and NP acknowledge support from NSF CAREER award 1455090. Part of the research was carried out at the Jet Propulsion Laboratory, California Institute of Technology, under a contract with NASA. MMK thanks Brian Metzger for providing us theoretical light curves for neutron-powered precursors. We thank the referee for constructive feedback.

## REFERENCES

- Aasi, J., et al. 2014, ApJS, 211, 7  
 Abbott, B., et al. 2016a,  
<https://dcc.ligo.org/LIGO-P1500227/public/main>

<sup>1</sup> <http://ptf.caltech.edu/ztf>

<sup>2</sup> <http://growth.caltech.edu>

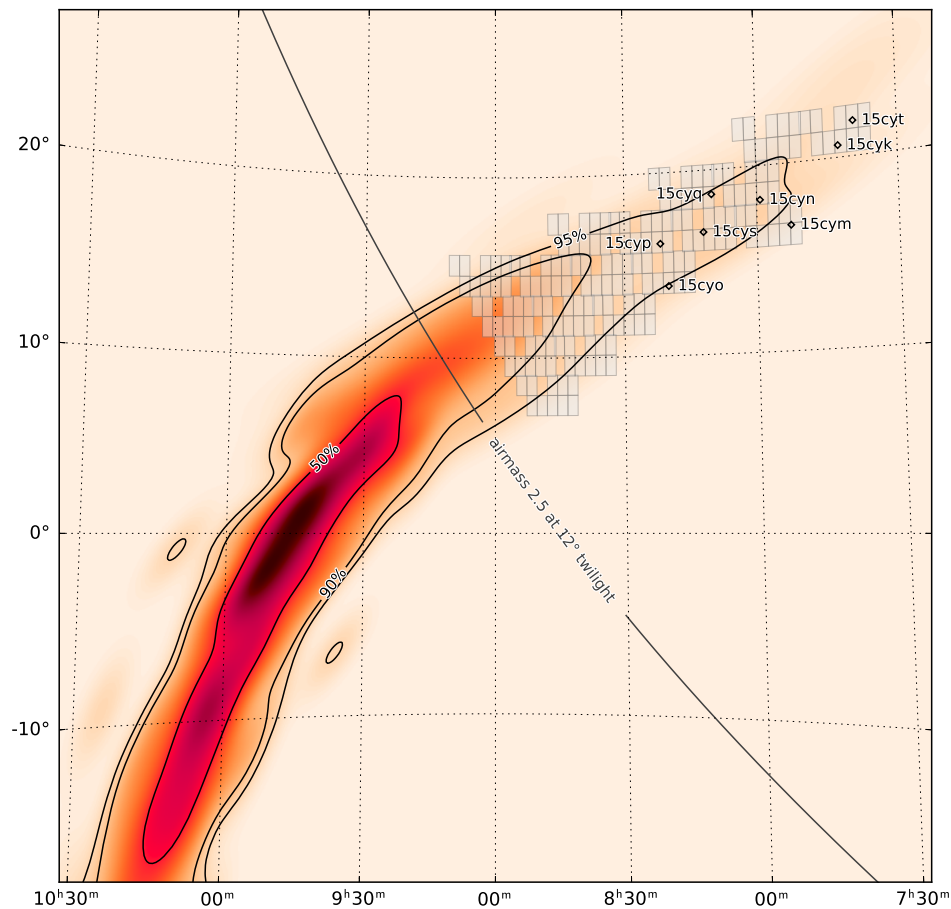


**Figure 1.** iPTF coverage map (gray tiles) of GW150914. The color coding and contours denotes GW probability. Due to the sun-angle and elevation constraints, we were only able to image the westernmost region of the localization. Eight candidates were identified and classified.

—. 2016b, *Physical Review Letters*, 116, 061102

Abbott, B. P., et al. 2013, *ArXiv e-prints*

Bellm, E. 2014, in *The Third Hot-wiring the Transient Universe Workshop*, ed. P. R. Wozniak, M. J. Graham, A. A. Mahabal, & R. Seaman, 27–33

Berry, C. P. L., et al. 2015, *ApJ*, 804, 114

Breeveld, A. A., Landsman, W., Holland, S. T., Roming, P., Kuin, N. P. M., & Page, M. J. 2011, in *American Institute of Physics Conference Series*, Vol. 1358, *American Institute of Physics Conference Series*, ed. J. E. McEnery, J. L. Racusin, & N. Gehrels, 373–376

Brink, H., Richards, J. W., Poznanski, D., Bloom, J. S., Rice, J., Negahban, S., & Wainwright, M. 2013, *MNRAS*, 435, 1047

Burrows, D. N., et al. 2005, *Space Sci. Rev.*, 120, 165

Evans, P. A., Kennea, J. A., Barthelmy, S. D., et al. 2016, *arXiv:1602.03868*

Faber, S. M., et al. 2003, in *Proc. SPIE*, Vol. 4841, *Instrument Design and Performance for Optical/Infrared Ground-based Telescopes*, ed. M. Iye & A. F. M. Moorwood, 1657–1669

Gehrels, N., et al. 2004, *ApJ*, 611, 1005

Howell, D. A., et al. 2005, *ApJ*, 634, 1190

Kasen, D., Fernández, R., & Metzger, B. D. 2015, *MNRAS*, 450, 1777

Kasen, D., & Bildsten, L. 2010, *ApJ*, 717, 245

Kasliwal, M. M. 2013, *Science*, 340, 555

Kasliwal, M. M., Cenko, S. B., Cao, Y., et al. 2015, *GCN*, 18341, 1

Kasliwal, M. M., & Nissanke, S. 2014, *ApJLetters*, 789, L5

Kulkarni, S. R. 2012, *ArXiv e-prints*

Law, N. M., et al. 2009, *PASP*, 121, 1395

Li, W., et al. 2011, *MNRAS*, 412, 1441

LIGO Scientific Collaboration, & Virgo. 2015, *GCN*, 18330, 1

—. 2016, *GCN*, 18858, 1

Masci, F. e. a. 2016, *PASP*

Metzger, B. D., Bauswein, A., Goriely, S., & Kasen, D. 2015, *MNRAS*, 446, 1115

Metzger, B. D., & Fernández, R. 2014, *MNRAS*, 441, 3444

Metzger, B. D., Vurm, I., Hascoët, R., & Beloborodov, A. M. 2014, *MNRAS*, 437, 703

Nicholl, M., Smartt, S. J., Jerkstrand, A., et al. 2014, *MNRAS*, 444, 2096

Nissanke, S., Kasliwal, M., & Georgieva, A. 2013, *ApJ*, 767, 124

Nugent, P., Cao, Y., & Kasliwal, M. M. 2015, in *Proc. SPIE*, Vol. 9397, *Visualization and Data Analysis*

Ofek, E. O., et al. 2013, *ApJ*, 763, 42

Palliyaguru, N., Corsi, A., et al. 2016, *GCN*, 18914, 1

Perley, R., et al. 2009, *IEEE Proceedings*, 97, 1448

Quimby, R. M., Kulkarni, S. R., Kasliwal, M. M., et al. 2011, *Nature*, 474, 487

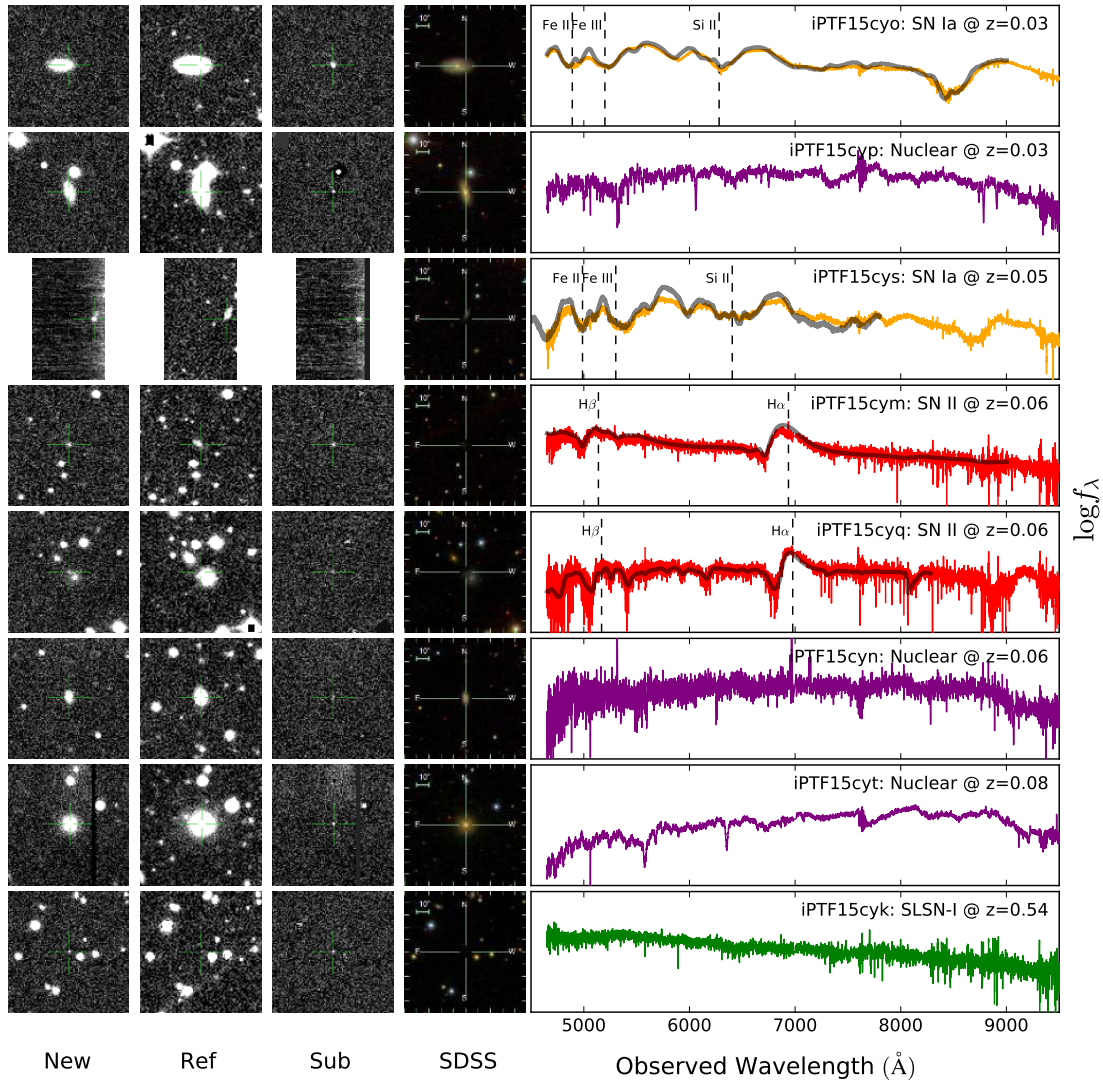


**Figure 2.** Keck II/DEIMOS classification spectra of eight iPTF candidates obtained within 2 hours of discovery. Also shown, from left to right, the P48 discovery image, reference image, subtraction image and SDSS thumbnail around each candidate location. Colors denote spectroscopic class: SN Ia (red), SN II (blue), Nuclear (purple), SLSN I (green). Overplotted in gray lines is the best match from a supernova spectra library (SN1996X for iPTF15cyo, SN2004eo for iPTF15cys, SN1999M for iPTF15cym, SN2004et for iPTF15cyq). Additional follow-up data was needed to classify iPTF 15cyk as a SLSN I (see Figure 5).

Quimby, R. M., Yuan, F., Akerlof, C., & Wheeler, J. C. 2013, *MNRAS*, 431, 912

Rana, J., Singhal, A., Gadre, B., Bhalerao, V., & Bose, S. 2016, arXiv:1603.01689

Rebbapragada, U. 2014, in *The Third Hot-wiring the Transient Universe Workshop*, ed. P. R. Wozniak, M. J. Graham, A. A. Mahabal, & R. Seaman, 205–205

Roming, P. W. A., et al. 2005, *Space Sci. Rev.*, 120, 95

Soares-Santos, M., Kessler, R., Berger, E., et al. 2016, arXiv:1602.04198

Singer, L. P., Kasliwal, M. M., Cenko, S. B., et al. 2015, *GCN*, 18337, 1

Singer, L. P., et al. 2013, *ApJLetters*, 776, L34

—. 2014, *ApJ*, 795, 105

—. 2015, *ApJ*, 806, 52

Smartt, S. J., Chambers, K. C., Smith, K. W., et al. 2016, arXiv:1602.04156

Connaughton, V., Burns, E., Goldstein, A., et al. 2016, arXiv:1602.03920

Zackay, B., Ofek, E. O., & Gal-Yam, A. 2016, *ArXiv e-prints*

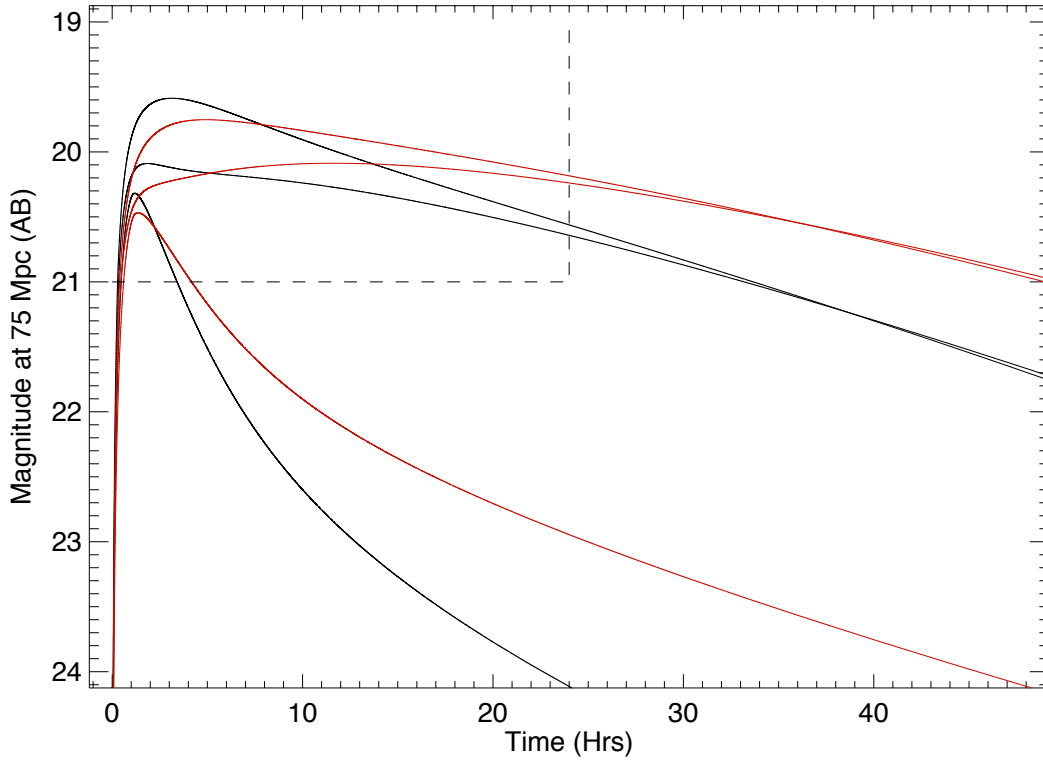


**Figure 3.** Predicted optical counterpart based on free neutron decay (Metzger et al. 2015). Black lines are g-band and red lines are r-band light curves at 75 Mpc (sensitivity limit of advanced LIGO to binary neutron star mergers in O1). The three curves assume three different values for opacity and neutron mass to represent the fast, intermediate and slow light curve evolution cases i.e. ( $\kappa_r = 30 \text{ cm}^2 \text{ gm}^{-1}$ ,  $M_n = 3 \times 10^{-5} M_\odot$ ), ( $\kappa_r = 3 \text{ cm}^2 \text{ gm}^{-1}$ ,  $M_n = 3 \times 10^{-5} M_\odot$ ), ( $\kappa_r = 3 \text{ cm}^2 \text{ gm}^{-1}$ ,  $M_n = 3 \times 10^{-4} M_\odot$ ). Note that g-band is more luminous at peak but decays faster. Horizontal dashed line denotes the sensitivity of iPTF in 60 s. Vertical dashed line denotes the timescale within which follow-up is undertaken by the GROWTH program.

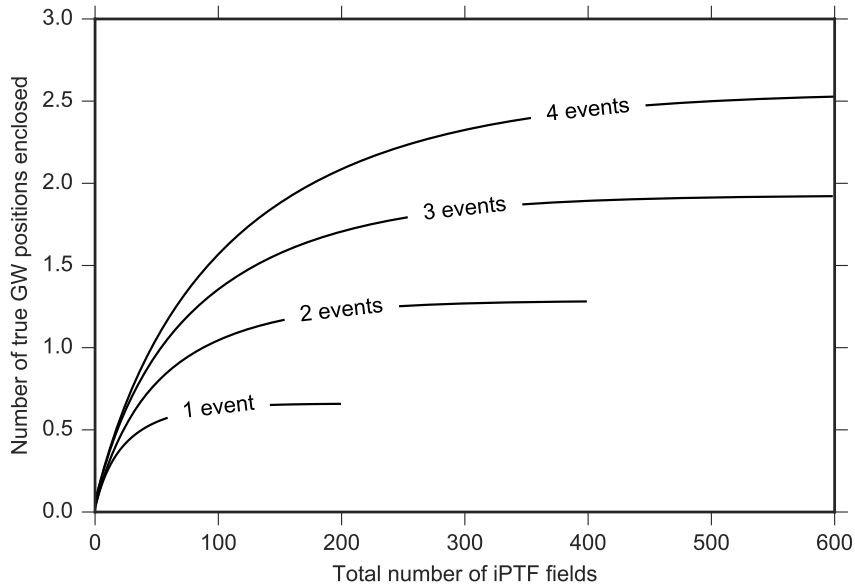


**Figure 4.** A simulation to compute the average number of times the true GW position would be enclosed in the iPTF imaged area as a function of the total number of iPTF fields imaged. Each iPTF field is  $7.1 \text{ deg}^2$  and two 60 s images of 150 fields can be obtained in a night. Thus, we need to follow-up 2 GW events to have at least 1 in our imaged area.



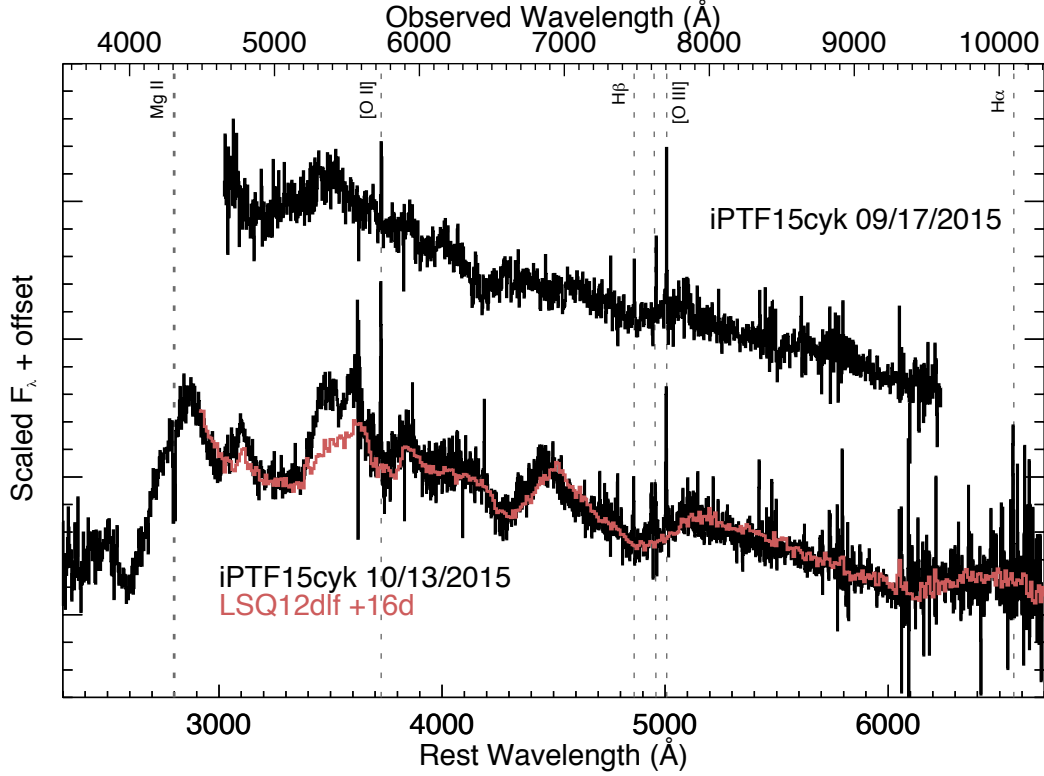


**Figure 5.** Spectral evolution of iPTF15cyk. The spectra show narrow lines from the host galaxy corresponding to  $z=0.539$ . The second spectrum matches a hydrogen-poor super luminous supernova, LSQ12dlf at +16d.

**Table 1.** Candidates Flagged for Follow-Up

Name	RA (J2000)	DEC (J000)	Discovery time	Mag (R-band)	Minutes to Spectrum	Classification	Redshift
iPTF15cyo	8h 19m 56.18s	+13d 52' 42.0"	2015-09-17 05:54:55.6	$17.75 \pm 0.01$	71	SN Ia (SN1996X-like, +23d)	0.029
iPTF15cyp	8h 21m 43.68s	+16d 12' 42.0"	2015-09-17 05:56:31.6	$19.48 \pm 0.05$	125	Nuclear	0.028
iPTF15cys	8h 11m 55.59s	+16d 43' 10.1"	2015-09-17 06:05:16.6	$17.84 \pm 0.03$	46	SN Ia (SN2004eo-like, +22d)	0.05
iPTF15cym	7h 52m 35.67s	+16d 45' 59.6"	2015-09-17 05:46:17.1	$19.88 \pm 0.20$	113	SN II (SN1999M-like, +5d)	0.055
iPTF15cyq	8h 10m 00.86s	+18d 42' 18.1"	2015-09-17 05:57:16.3	$20.05 \pm 0.10$	39	SN II (SN2004et-like, +47d)	0.063
iPTF15cyn	7h 59m 14.93s	+18d 12' 54.9"	2015-09-17 05:47:20.5	$20.34 \pm 0.28$	124	Nuclear	0.062
iPTF15cyt	7h 38m 59.35s	+21d 45' 43.2"	2015-09-17 06:08:09.3	$19.65 \pm 0.09$	82	Nuclear	0.078
iPTF15cyk	7h 42m 14.87s	+20d 36' 43.4"	2015-09-17 05:38:38.3	$20.28 \pm 0.12$	97	SLSN I (LSQ12dlf-like, +16d)	0.539

**Table 2.** Panchromatic follow-up of super luminous supernova iPTF15cyk

Facility	Epoch UTC	Frequency	Flux Limit $\text{erg cm}^{-2} \text{s}^{-1} \text{Hz}^{-1}$
Swift/XRT	18 Sep 2015 18:12	2 keV	$< 4.5 \times 10^{-32}$
VLA	15 Oct 2015 11:20:32-12:05:27	5.43 GHz	$< 2.6 \times 10^{-28}$
VLA	06 Dec 2015 04:52:11-05:00:07	5.43 GHz	$< 2.3 \times 10^{-28}$
VLA	20 Jan 2016 01:55:31-02:59:40	5.43 GHz	$< 2.3 \times 10^{-28}$

**Table 3.** Observations Log

PTF Field ID	Central RA (J2000)	Central DEC (J2000)	Observation Time (UTC)	Filter	Airmass	Limiting mag ( $5\sigma$ )
3050	132	7.875	2015-09-17 12:13:20.041	R	2.7	20.4
3050	132	7.875	2015-09-24 12:02:27.041	R	2.3	20.3
3050	132	7.875	2015-09-24 12:13:29.89	R	2.1	20.3
3154	129.80769	10.125	2015-09-17 12:11:38.141	R	2.4	20.4
3155	133.26923	10.125	2015-09-17 12:15:01.341	R	2.	20.2
3257	127.57282	12.375	2015-09-17 12:03:09.29	R	2.3	20.6
3257	127.57282	12.375	2015-09-17 12:33:41.591	R	1.	19.6
3258	131.06796	12.375	2015-09-17 12:09:56.041	R	2.4	20.4
3258	131.06796	12.375	2015-09-17 12:40:29.29	R	1.9	18.2
3259	134.56311	12.375	2015-09-17 12:16:43.241	R	2.6	20.1
3359	125.29412	14.625	2015-09-17 12:01:27.441	R	2.1	20.6
3359	125.29412	14.625	2015-09-17 12:32:00.191	R	1.7	20.0
3360	128.82353	14.625	2015-09-17 12:04:51.39	R	2.2	20.5
3360	128.82353	14.625	2015-09-17 12:35:23.591	R	1.8	19.3
3361	132.35294	14.625	2015-09-17 12:08:14.941	R	2.4	20.4
3361	132.35294	14.625	2015-09-17 12:38:46.99	R	1.9	18.6
3362	135.88235	14.625	2015-09-17 12:18:25.191	R	2.5	20.2
3459	119.40594	16.875	2015-09-17 11:52:55.541	R	1.8	20.8
3459	119.40594	16.875	2015-09-17 12:23:31.44	R	1.5	20.7
3459	119.40594	16.875	2015-12-03 09:36:36.833	g	1.0	20.8
3459	119.40594	16.875	2015-12-03 10:25:33.583	g	1.0	20.8
3459	119.40594	16.875	2015-12-09 08:44:28.483	g	1.1	19.6
3459	119.40594	16.875	2015-12-09 09:25:19.082	g	1.0	20.7
3459	119.40594	16.875	2015-12-15 09:16:17.383	g	1.0	21.1
3460	122.9703	16.875	2015-09-17 11:56:20.941	R	1.	20.6
3460	122.9703	16.875	2015-09-17 12:26:54.891	R	1.6	20.4
3461	126.53465	16.875	2015-09-17 11:59:45.941	R	2.	20.6
3461	126.53465	16.875	2015-09-17 12:30:18.641	R	1.7	20.1
3461	126.53465	16.875	2015-09-18 11:39:19.14	R	2.4	20.6
3461	126.53465	16.875	2015-09-18 12:00:28.941	R	2.0	20.7
3462	130.09901	16.875	2015-09-17 12:06:33.19	R	2.2	20.6
3462	130.09901	16.875	2015-09-17 12:37:05.491	R	1.8	19.0
3560	120.6	19.125	2015-09-17 11:54:37.991	R	1.8	20.8
3560	120.6	19.125	2015-09-17 12:25:12.741	R	1.5	20.6
3560	120.6	19.125	2015-09-18 11:13:55.441	R	2.3	20.6
3560	120.6	19.125	2015-09-18 11:37:37.341	R	1	20.7
3560	120.6	19.125	2015-12-03 09:38:18.533	g	1.0	20.8
3560	120.6	19.125	2015-12-03 10:27:16.483	g	1.0	20.9
3560	120.6	19.125	2015-12-09 08:46:08.433	g	1.1	19.4
3560	120.6	19.125	2015-12-09 09:26:59.082	g	1.0	20.5
3560	120.6	19.125	2015-12-15 09:17:59.533	g	1.0	21.1
3561	124.2	19.125	2015-09-17 11:58:03.64	R	1.9	20.7
3561	124.2	19.125	2015-09-17 12:28:36.291	R	1.6	20.4
3561	124.2	19.125	2015-12-03 09:46:51.133	g	1.0	20.8
3561	124.2	19.125	2015-12-03 10:35:47.883	g	1.0	20.8
3561	124.2	19.125	2015-12-09 09:35:19.683	g	1.0	21.0
3561	124.2	19.125	2015-12-15 09:26:36.183	g	1.	21.1
3658	115.71429	21.375	2015-09-17 11:49:31.191	R	1.6	20.9
3658	115.71429	21.375	2015-09-17 12:20:07.791	R	1.4	20.9
3658	115.71429	21.375	2015-09-18 10:50:48.89	R	2.3	20.6
3658	115.71429	21.375	2015-09-18 11:12:13.34	R	2.0	20.7
3658	115.71429	21.375	2015-09-19 11:44:38.64	R	1.6	20.7
3658	115.71429	21.375	2015-09-19 12:26:26.091	R	1.3	20.8
3658	115.71429	21.375	2015-12-03 09:26:08.832	g	1.0	20.8
3658	115.71429	21.375	2015-12-03 10:14:56.283	g	1.0	20.9
3658	115.71429	21.375	2015-12-09 08:41:08.233	g	1.1	19.3